SEDIMENT FLOW CHARACTERISTICS ON SEABED SUBJECTED TO STATIONARY WAVES WITH DIAGONAL INCIDENT WAVE LOADING NEAR LINE STRUCTURES

*Anh Quang TRAN[1], Kinya MIURA[2], Tatsuya MATSUDA[3] and Takahito YOSHINO[4]

[1,4]Graduate School of Architecture and Civil Engineering, Toyohashi University of Technology, Japan
[2,3]Department of Architecture and Civil Engineering, Toyohashi University of Technology, Japan

ABSTRACT: Typical stationary waves are caused by overlapped the incident and reflected wave, when the plane wave vertically meets a line structure. In this case characteristic sediment flow behavior is observed and seabed is suffered from configuration change such as erosion and deposition. In more general situations where plane wave meets line structures in diagonal direction, however, overlapped waves would behave in three-dimensional manner. The stability of structures subjected to stormy ocean waves or tsunami depends on the integrity of seabed foundation ground, as well as the wave pressure acting directly on the structures. Thus, reliable analysis method for evaluating the sediment flow on seabed and associated erosion-deposition is needed. The present study aims to clarify the sediment flow characteristics induced by the diagonal incident and reflected waves which meet line structure and broken line structure, with seabed effective stress response to sea wave loading into account. Erosion-deposition behavior was quantitatively examined based on the calculated results.

Keywords: Erosion-deposition behavior, Effective stress response, Linear wave theory, Traction flow

1. INTRODUCTION

Because the stability of structure subjected to ocean waves depends on not only wave force, but also on seabed which support it, reasonable analysis method of the deformation of seabed induced by sediment flow is needed.

The scour phenomenon is evaluated in the forms of the sheet flow, the suspended load transport, and the bedload transport, etc. caused as a function of the flow velocity at the seabed. On the other hand, the stability of the structures is sometimes affected by the effective stress change in seabed [1]. From the geotechnical point of view, seabed is modeled as a continuum, and the effective stress response to the pressure variation is calculated [2,3].

In the present study, we propose an analysis method for evaluating sediment flow regarding the response of effective stress to wave loading. Miura, Morimasa, Otsuka, Yamazaki and Konami [4] qualitatively examined the characteristic sediment flow under traveling wave, stationary wave, and irregular wave. In this study, we quantitatively examine the sediment flow behavior near line structures including broken line structure with right angle corner.

2. ANALYSIS METHOD

The analysis method used consists of a wave analysis with linear wave theory, an effective stress analysis with a poro-elastic model, and an empirical evaluation of sediment flow quantity by tractive force.

2.1 Wave Analysis

Velocity potential was derived within the frame of the linear wave theory, and an incident wave and associated reflected waves were superimposed. In the analysis the seabed was assumed to be uniform, infinite in depth, and impermeable.

When wave travels along *x*-axis, the water surface and the velocity potential are presented by Eq. (1a, b) for the plane wave with wave height of H, wavelength of L, and period of T. The velocity potential function was modified for the traveling wave in an arbitrary direction by Eq. (2). The velocity components and water pressure can be calculated as the derivatives of the velocity potential function.

$$\eta(x, y, t) = \frac{H}{2} e^{i(\lambda x - \omega t)} \quad \because \lambda = \frac{2\pi}{L}, \quad \omega = \frac{2\pi}{T} \quad (1a)$$

$$\phi(x, y, z, t) = i \frac{gH}{2\omega} \frac{\cosh\lambda(h+z)}{\cosh\lambda h} e^{i(\lambda x - \omega t)} \quad (1b)$$

$$\phi = i \frac{gH}{2\omega} \frac{\cosh\lambda(h+z)}{\cosh\lambda h} e^{i(\lambda x \cos\alpha + \lambda y \sin\alpha - \omega t)} \quad (2)$$

$$\because x \to x\cos\alpha + y\sin\alpha$$

$$v_i = -\phi_i, \quad p = \rho_w(\dot{\phi} - gz) \qquad (3)$$

2.1.1 Reflection at line structure

When the plane wave meets a line structure at an angle of $\alpha_i = \alpha$, the traveling direction angle of the reflected wave becomes $\alpha_r = 180° - \alpha$ as shown in Fig. 1(a). Thus, the overlapping wave is expressed by Eq. (4) from the boundary condition ($v_x = 0$ at $x = 0$). The wave height of the overlapping wave becomes $2H$. Both of the characteristics of stationary wave and traveling wave are recognized in x-direction and y-direction, respectively, where wavelengths along coordinate axes are expressed by Eq. (5).

$$\phi = \phi_i + \phi_r = i\frac{gH}{\omega}\frac{\cosh\lambda(h+z)}{\cosh\lambda h} \qquad (4)$$
$$\times \cos(\lambda x \cos\alpha)e^{i(\lambda y \sin\alpha - \omega t)}$$

$$L_x = L/\cos\alpha, \quad L_y = L/\sin\alpha \qquad (5)$$

2.1.2 Reflection at broken line structure

As shown in Fig. 1(b, c), we considered a plane wave which meets broken line structure. The part of the incident wave in right hand side of coordinate origin is first reflected on y-axis (reflected wave r_y) and then on x-axis (reflected wave r_{yx}). The other part of the incident wave in left hand side is reflected first on x-axis (reflected wave r_x) and then on y-axis (reflected wave r_{xy}). From the boundary condition ($v_x = 0$ at $x = 0$; $v_y = 0$ at $y = 0$), the traveling direction angle of this reflected wave and the velocity potential of the overlapping wave can be expressed as follows.

$$\alpha_i = \alpha, \quad \alpha_{ry} = 180° - \alpha, \quad \alpha_{rx} = -\alpha,$$
$$\alpha_{ryx} = \alpha_{rxy} = 180° + \alpha \qquad (6)$$

$$\phi = \phi_i + \phi_{ry} + \phi_{rx} + \phi_{ryx} = i\frac{2gH}{\omega}\frac{\cosh\lambda(h+z)}{\cosh\lambda h} \qquad (7)$$
$$\times \cos(\lambda x \cos\alpha)\cos(\lambda y \sin\alpha)e^{-i\omega t}$$

The reflected wave r_{yx} and the reflected wave r_{xy} are opposite to the incident wave. The characteristics of the stationary wave can be recognized both in x- and y-directions. The node appears on the rectangular grid, but the loop appears at the center of the grid including the coordinate origin. Wavelengths are the same as those in Eq. (5).
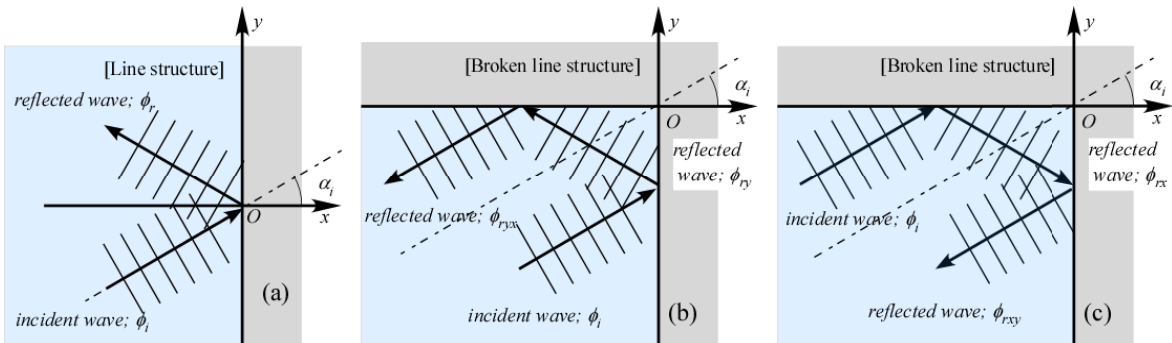

Fig. 1   Reflection of diagonal incident waves. (a) line structure;
(b), (c) broken line structure: (b) y-x reflection, (c) x-y reflection

2.2 Effective Stress Response Analysis of the Seabed

The effective stress response in seabed to wave loading was analyzed by using poro-linear-elastic model [2]. The simultaneous differential equations which are derived for porous solid phase formed with soil particles and fluid phase including averaged pore water and pore air, are formulated in the model. Miura, Asahara, Otsuka and Ueno [5] examined the applicability of formulation under the wide conditions, according to which we employed the u-p formulation under quasi-dynamic, one-dimensional condition. For the homogeneous seabed, when the boundary condition is taken in infinite depth, the component of variation of the pore water pressure and the effective stress are computable by Eq. (8). E_u, B_f are the modulus of rigidity of the solid phase, the liquid phase, respectively, and complex parameter ζ is related with coefficient of hydraulic consolidation h_v (s/m^2) in Eq. (9) [5].

$$\Delta p(z,t) = \Delta p_o \frac{1}{B_f + E_u}(B_f + E_u e^{-\zeta z})e^{-i\omega t}$$

$$\Delta\sigma_z(z,t) = \Delta p_o \frac{E_u}{B_f + E_u}(1 - e^{-\zeta z})e^{-i\omega t} \qquad (8)$$

$$\because \Delta p_o e^{-i\omega t} = \rho_w\dot{\phi} \quad \text{at } z = -h \text{ (on seabed surface)}$$

$$\zeta = \sqrt{i\omega h_v} \qquad (9)$$

2.3 Calculation of Sediment Flow and Storage

Based on the idea of the Shields number, we evaluated the amount of sediment flow. First, the shear stress acting on the seabed was evaluated as a function of seawater flow velocity. Next, the thickness of sediment shear flow layer was decided from frictional resistance related to the effective stress in seabed ground. Then triangular flow velocity was assumed within the shear flow layer. Storage was calculated from the balance of inflow and out flow of infinitesimal area.

2.3.1 Sediment flow amount

The shear stress, tractive force per specific seabed surface area, was assumed to be proportional to the seawater flow velocity squared. We employed Eq. (10), where dimensionless coefficient C_b was assumed to be 1/40.

$$\tau_b = C_b \rho_w v_b^2 \ (\mathrm{N/m^2}) \qquad (10)$$

It was assumed that the sediment fluidization is mobilized within the layer of d_f in thickness where shear stress τ_b exceeds shear resistance τ_f which is calculated as a function of effective stress σ_z and internal friction angle ϕ as shown in Eq. (11). Finally we could determine the fluidization depth d_f(m).

$$\tau_f = \sigma_z(z)\tan\phi \ (\mathrm{kN/m^2}) \qquad (11)$$

$$\tau_b = \tau_f \Rightarrow z = d_f \ (\mathrm{m}) \qquad (12)$$

It was assumed that the distribution of sediment flow velocity v_f in the fluidization layer is triangular along depth as shown in Fig. 2. Thus, the amount of sediment flow per unit width q was calculated by Eq. (13). The dimensionless coefficient C_q was introduced for the difference between seawater flow velocity v_b and sediment flow velocity v_f; the value of C_q was assumed to be 1/2.5.

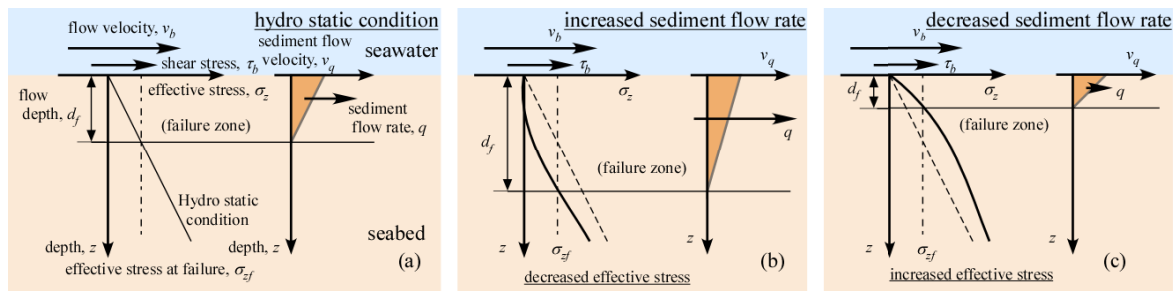$$q = \frac{1}{2}d_f v_f = \frac{1}{2}d_f C_q v_b \ (\mathrm{m^2/s}) \qquad (13)$$

Fig. 2   Sediment flow behavior: (a) hydrostatic pressure condition,
(b) effective stress decrease condition, (c) effective stress increase condition

2.3.2 Sediment storage rate: erosion and deposition

As shown in Fig. 3, the rate of sediment storage designated as Q can be calculated from the total balance of inflow and out flow in both x- and y-directions of an infinitesimal rectangular area. The storage rate Q is a function of coordinates as well as time in Eq. (14); Q is a summation of the derivatives of q in x- and y-directions.

$$Q = -\frac{q_{x(x+\Delta x/2,y)} - q_{x(x-\Delta x/2,y)}}{\Delta x}$$

$$-\frac{q_{y(x,y+\Delta y/2)} - q_{y(x,y-\Delta y/2)}}{\Delta y} \qquad (14)$$

$$\rightarrow -\left(\frac{\partial q_x}{\partial x} + \frac{\partial q_y}{\partial y}\right) \ (\Delta x \rightarrow 0, \Delta y \rightarrow 0) \ (\mathrm{m/s})$$

The positive and negative values of sediment storage rate Q correspond to deposition and erosion, respectively. The sediment flow velocity q and storage rate Q both can be integrated during a sea wave period T for evaluating the total behavior of sediment flow; the integration values were defined as q_T (m²) and Q_T (m), respectively.
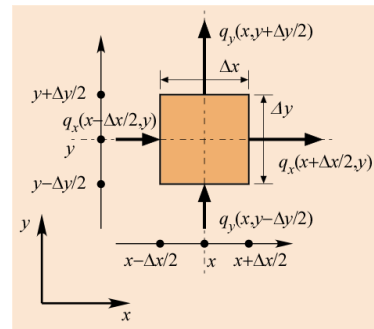

Fig. 3   Calculation of the sediment storage from the balance of inflow and out flow

3. WAVE CONDITION AND GROUND MATERIAL PROPERTIES

Seawater with uniform depth of $h = 20$m is assumed. The period of incident wave is $T = 13$s (wavelength $L = 167.5$m), and wave height is $H = 10$m; H was parametrically changed. The Japanese Coastal Engineering Committee in Japan Society of Civil Engineers organized the intensive study with several researchers on the effective stress response in seabed ground to sea wave loading [6]. In the present study we selected physical and mechanical properties of seabed material as well as sea wave condition according to the committee report. The properties determined for typical loose sand was employed (as shown in Table 1), because the loose sand shows the notable effective stress response compared with other types of soils, such as gravel, silt, and clay [6].

Table 1 Mechanical properties of loose sand

E_u: Stiffness of solid phase (kN/m^2)	1.40×10^5
B_f: Stiffness of pore fluid phase (kN/m^2)	0.93×10^5
h_v: Coefficient of hydraulic consolidation (s/m^2)	1.75×10^{-3}

4. EXAMINATION OF CALCULATED BEHAVIOR AND DISCUSSION

4.1 Line Structure with Perpendicular Incident Wave

First, the case where the plane wave travels onto a line structure is examined. Figure 4 shows the sediment flow behavior per a period over a wavelength; the wave height H is changed from 10m to 2m parametrically. Short dashed line is for sediment flow amount q_{Tx} and the solid line for sediment storage Q_T per period. The variation of sediment flow q_{Tx} is skew-symmetric with respect to two nodes ($x/L = -6/8$, $-2/8$); this behavior suggests that sediment flow into the nodes in both left- and right-hand directions. As a result, the storage Q becomes positive at the nodes. On the other hand, Q becomes negative at loops ($x/L = -8/8$, $-4/8$, $0/8$). This behavior suggests that sediment is deposited at the nodes, while seabed is eroded at the loops including the line structure side. As the wave height H becomes lower, the characteristic sediment flow behavior becomes not clear, and sediment tends to deposit at points a little distant from the nodes.

Figure 5 shows the form of the entire stationary wave, and the relation between water pressure and flow velocity on the seabed surface at
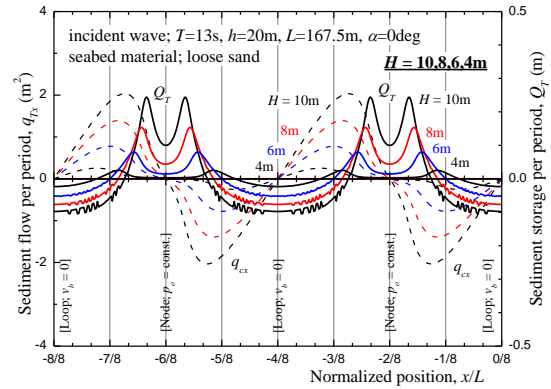

Fig. 4 Sediment flow behavior when wave meets perpendicularly to line structure
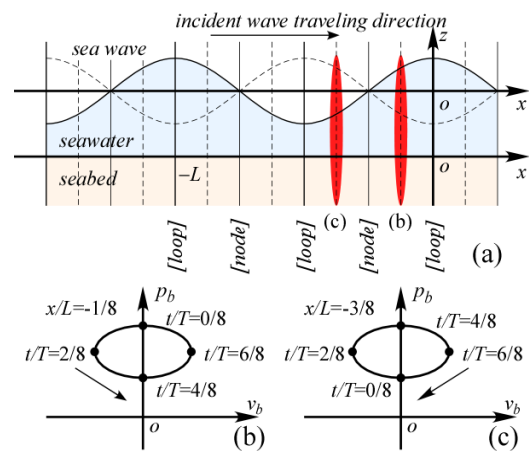

Fig. 5 Schematic explanation of the stationary wave perpendicular to line structure: (a) formation of wave; relation of water pressure vs. flow velocity on seabed (b) $x/L = -1/8$, (c) $x/L = -3/8$

the mid-points ($x/L = -1/8$, $-3/8$) between the node and loop.

In addition, Figs. 6, 7 show schematically the behavior of the sediment flow at the mid-points. In the period of sea wave, a decrease in water pressure p on seabed surface causes effective stress to decrease and become less than the hydrostatic state. As a result, the fluidization depth d_f becomes deeper during the decrease of p. As shown in Fig. 6, at the mid-point on right hand side of the node ($x/L = -1/8$) the sediment flow in negative direction is accelerated ($t/T = 2/8$). On the other hand, at the mid-point on left hand side of the node ($x/L = -3/8$) the sediment flow in positive direction is accelerated ($t/T = 6/8$) as shown in Fig. 7. Finally, under the influence of effective stress response, sediment moves toward to the node from both sides. This behavior is clearly shown by the variation in the storage per period Q_T; at the nodes, Q_T becomes positive meaning cumulative deposition, and at the loops it becomes negative meaning cumulative erosion.
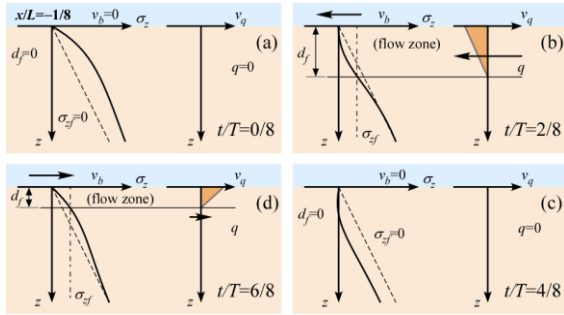
Fig. 6 Negative sediment flow at mid-point between node and loop ($x/L = -1/8$): (a-d) $t/T = 0/8$, 2/8, 4/8, 6/8
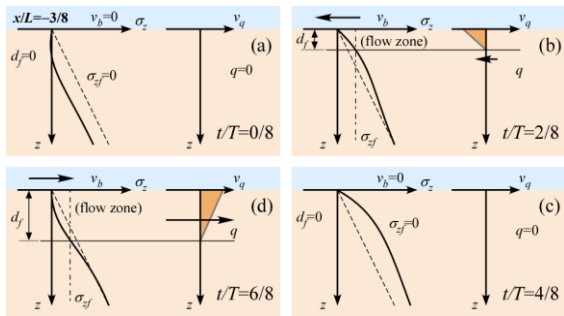

Fig. 7 Positive sediment flow at mid-point between node and loop ($x/L = -3/8$): (a-d) $t/T = 0/8$, 2/8, 4/8, 6/8

4.2 Line Structure with Diagonal Incident Wave

In the case where a plane wave ($H = 10$m) meets line structure with $\alpha = 30°$, the sea surface level at $t/T = 0$ is indicated by contour lines and color gradation, and the horizontal velocity by vectors in Fig. 8. Along the node lines sea surface does not fluctuate vertically, but horizontally. One can recognize the characteristics of stationary wave in x-axis direction, and those of traveling wave in y-axis direction as in Eq. (4), (5).
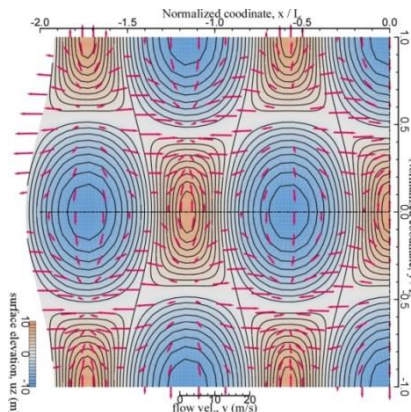

Fig. 8 Water level and flow velocity on sea surface near line structure

Figure 9 shows the sediment flow per period q_T

by vectors, and the storage by contour lines and color gradation. In this condition, because the characteristics of the stationary wave appear only in x-axis direction, the node lines and loop lines are parallel to the y-axis. The erosion and deposition of sediment occur within narrow bands parallel to y-axis. In the y-axis direction, the vectors q_T are heading to the opposite direction of wave traveling.
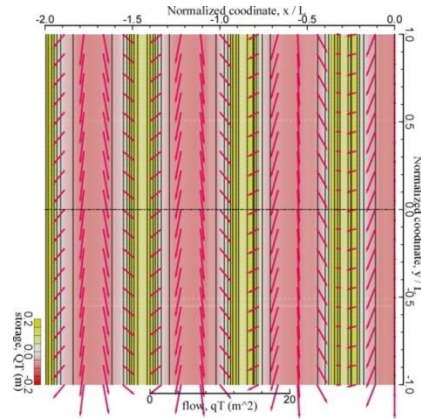

Fig. 9 Sediment flow, erosion-deposition behavior per period near line structure

4.3 Broken Line Structure with Diagonal Incident Wave

In the case where a plane wave ($H = 5$m) meets broken line structure with $\alpha = 30°$, the behavior of the sea surface at $t/T = 0$ is shown in Fig. 10; the elevation of sea surface is indicated by contour lines and color gradation, and horizontal velocity by vectors. The characteristics of stationary wave are recognized in both x- and y-directions as shown in Eq. (5), (7). Nodes appear along the grid lines, and loops at the center of the rectangular grid cells. As shown in Figs. 8, 9, in the case of the line structure, nodes do not appear along structure independently of incident wave angle; however, in the case of the broken line structure, loops and nodes both appear periodically along the structure.
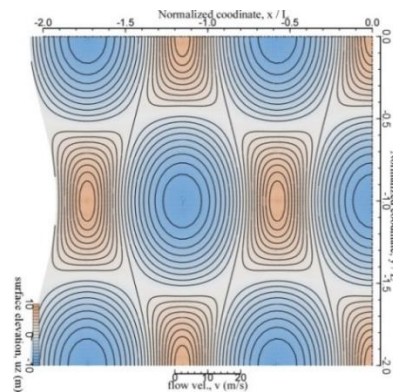

Fig. 10 Water level and flow velocity on sea surface near broken line structure

Figure 11 shows the sediment flow per period q_T by vectors, and the sediment storage per period Q_T by contour lines and color gradation. The sediment is eroded near the loop points, and deposited on the node lines. It is notable that at the corner of the broken line structure, seabed sediment is eroded, and sediment is deposited and eroded periodically along the sides of the structure.
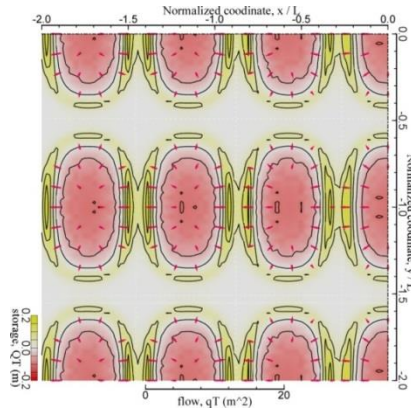

Fig. 11 Sediment flow, erosion-deposition behavior per period near broken line structure

4.4 Influence of Incident Wave Direction on Sediment Erosion-deposition Behavior

For both the line structure and the broken line structure, the erosion (negative storage per period) at the loops (including coordinate origin) and the deposition (positive storage per period) at the nodes are plotted against the incident angle in Fig. 12. The deposition at node monotonously decreases with the increase of incident angle α. It is notable that the difference of amount of deposition between the line structure and broken line structure is not recognized. It is clear that in the line structure, the amount of erosion at loop gradually decreases, as α increases. In the broken line structure, however, the erosion amount at the loop is constant independently of α.
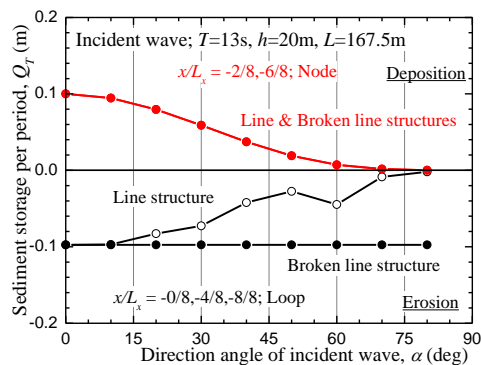

Fig. 12 Influence of incident angle of wave on erosion-deposition of sediment

5. CONCLUSION

We explained the analysis method for the traction sediment flow induced by traveling wave and stationary waves that meet line structures. We can summarize findings in the quantitative examination of the calculation results.

Under the traveling wave sediment flow occurs in opposite direction to wave traveling direction, and neither erosion nor deposition occurs. The characteristics of stationary wave appeared only in perpendicular direction in the case of line structures, but in both perpendicular directions in the case of broken line structures. Under the stationary waves, sediment is eroded near loops, and deposited near nodes.

6. ACKNOWLEDGEMENTS

7. REFERENCES

[1] Oka F., Yashima A., Miura K., Ohmaki S. and Kamata A., Settlement of Breakwater on Submarine Soil Due to Wave-induced Liquefaction, 5th ISOPE, Vol.2, 1995, pp.237-242.

[2] Yamamoto T., H. S. L. Koning and E. Van Hijum, On the Response of a Pore-elastic Bed to Water Waves, J. of Fluid Mechanics, Vol. 87, Part 1, 1978, pp.193-206.

[3] Zen K. and Yamazaki H., Mechanism of wave-induced liquefaction and densification in seabed, Soils and Foundations, Vol.30, No.4, 1990, pp.90-104.

[4] Miura K., Morimasa S., Otsuka N., Yamazaki H. and Konami T., Combined Effect of Flow Velocity and Water Change on Wave-induced Seabed Destabilization, J. of Japan Society of Civil Engineers, Ser. B2 (Coastal Engineering), Vol. 66, Issue 1, 2010, pp.851-855 (in Japanese).

[5] Miura K., Asahara S., Otsuka N. and Ueno K., Formulation of The Ground for Coupled Analysis of The Seabed Response to The Wave, Proceedings of Symposium on Geotechnical Engineering, Vol. 49, 2004, pp.233-240 (in Japanese).

[6] Coastal Engineering Committee, Coastal Wave, Japan Society of Civil Engineers, 1994, pp.430-503 (in Japanese).